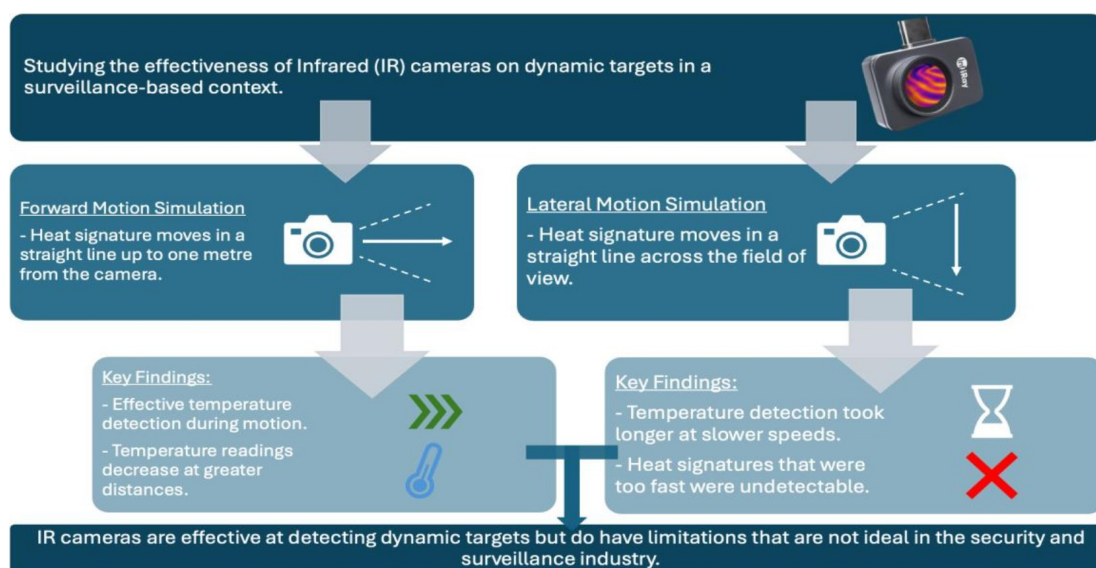


Evaluating Infrared Camera Performance in Detecting Moving Heat Signatures

Alysha Whitehouse¹, Bertie Lynch¹, George Ing¹, Samara Jirsa¹, Tom Waugh¹, Sebastian Dominguez Flores¹, Sebastian Dominguez Flores¹, Minghao Zhang¹, David Alam¹, Gobinath Rajarathnam¹

School of Chemical and Biomolecular Engineering, The University of Sydney, Australia

Graphical Abstract



Abstract

The development and widespread adoption of infrared (IR) cameras, capable of detecting static and dynamic heat signatures, have enabled the creation of advanced security and surveillance systems. While most of the current research into the effectiveness of IR cameras in security-based settings involves the use of static heat signatures, an understanding of how these cameras perform on dynamic targets is also vital as moving heat signatures are ubiquitous in real-world scenarios. This study aims to determine the efficacy of IR cameras on a heat signature in a range of different motions to justify or challenge their prevalent use in commercial and residential surveillance systems. In this research, both forward motion and lateral motion setups were used consisting of a one-meter straight path, in-line with the IR camera, and a 70 cm straight path, facing the IR camera side-on, respectively. Both experimental setups tested the heat signatures moving at multiple speeds. This study found in the forward motion test that the IR camera was accurate in observing the temperature of the heat signature, however, greater distances between the heat signature and the camera resulted in lower temperature recordings. The lateral motion test found the sense time for the heat signature increased as its speed decreased, and that there is a speed great enough at which the heat signature remains undetected by the IR camera. Consequently, this research has confirmed that limitations do exist in IR camera surveillance technology, meaning that while significantly effective, these systems cannot be completely relied upon.

Keywords: infrared camera, heat signatures, dynamic targets, security, surveillance, forward motion, lateral motion.

1. Introduction

1.1 Motivation

Heat transfer is defined as the movement of thermal energy, in the form of heat, between physical systems with different temperatures. This transfer can occur through three primary mechanisms: conduction, which involves molecular agitation within a material without any bulk motion of the substance; convection, the transfer through the movement of fluid or gas currents between bodies; and radiation, the transfer of energy through electromagnetic waves, which does not require a physical medium (Biosystems Heat and Mass Transfer - ScienceDirect, n.d.). All these modes of transfer operate under the same fundamental principle — the tendency toward thermodynamic equilibrium — whereby two objects at initially different temperatures in thermal contact will eventually reach the same temperature (Heat Transfer, n.d.). Subsequently, heat transfer from one body to another affects the temperature of each object and thereby alters the infrared (IR) radiation emitted, also known as the ‘heat signature’ (Thermal Sensors - Department of Informatics, n.d.). This heat exchange impacts not only the thermal state of each object but also the intensity of the emitted infrared radiation (Infrared Radiation - an Overview | ScienceDirect Topics, n.d.). Such radiation can be converted into visible images that depict the spatial distribution of temperature differences in a scene observed by a thermal (IR) camera (Havens & Sharp, 2016). These IR cameras operate similarly to visible light (VIS) cameras: electromagnetic radiation from objects passes through a lens system (and possibly additional optical components) before forming an image of the object on a detector (Vollmer, 2021). Originally developed as surveillance and night vision tools for military use (Gade & Moeslund, 2014), thermal cameras have since been commercialised due to decreased manufacturing costs and technological advancements, now serving broader applications in sectors such as agriculture, building inspection, gas detection, and other fields related to heat energy and air conditioning (Krišto, 2016). However, while thermal cameras are widely used in these static diagnostic applications, their effectiveness in dynamic surveillance scenarios—particularly for detecting and measuring the heat signature and temperature of moving objects—remains insufficiently explored. This article aims to assess how effectively thermal surveillance cameras can detect and measure a radiating moving object’s heat signature and temperature.

1.2 Literature Review

Detection of humans is the first step in many surveillance applications, and as such, general-purpose systems should be robust. For wide-area surveillance and tracking applications,

Leykin and Hammoud (2016) describe a tracking framework that integrates colour and thermal imagery using a Bayesian approach based on particle filtering. In their method, each object (human) is represented by a bounding box location and a 2D colour histogram, allowing for robust tracking across varying conditions (Bhusal, n.d.). Similarly, Zin et al. (2007) proposed a system for human detection, based on the extraction of the head region, and Davis and Sharma (2004) proposed a detection system that uses background subtraction, gradient information, watershed algorithm and A* search to robustly extract the silhouettes

Although prior research demonstrates the potential of combining thermal and visual data for robust tracking, few studies isolate and evaluate the standalone performance of thermal cameras in detecting moving radiating objects, revealing a gap that this research aims to address.

2. Experimental Method

2.1 Forward Motion Procedure

To assess the thermal signature generated during forward motion, a one-metre straight-line path was marked on a flat surface in a location that allowed unobstructed movement of the heat pack. The InfiRay thermal imaging camera was positioned 23 cm laterally from the zero point and angled such that the entire interval remained within the field of view throughout each trial. This distance ensured complete visibility of the heat pack at both the starting and ending positions. The heat pack, heated to approximately 50 °C, was aligned so that its centre coincided with the zero point. It was then moved smoothly along the path until its centre reached the one-metre mark. This motion was executed over three fixed durations: 10, 5, and 2.5 seconds, with three separate trials conducted for each time interval to ensure repeatability.

Before recording, the camera’s point temperature tool was configured to track maximum and minimum temperatures in each frame. This tool was adjusted to monitor the area occupied by the heat pack across the path while avoiding background interference. While continuous recording was possible, individual recordings were taken for each trial to simplify data management and to allow the exclusion of inaccurately timed or inconsistent runs.

2.2 Lateral Motion Procedure

The camera was fixed in a side-on position to ensure the entire heat pack remained completely visible as it moved across a 70 cm path perpendicular to the camera’s field of view. The camera was located 1.1 meters away from the centre of the heat packs traverse path. Eight sense points were designated at 10 cm intervals along this path, including the start and end positions, using the camera’s point temperature function to enable consistent spatial

temperature measurements. The midpoint sense point (P3) was selected for detailed analysis due to its central location and relatively stable background temperature. A temperature spike at P3 was defined as a frame-to-frame increase exceeding 3°C, surpassing the

cameras reported $\pm 2^\circ\text{C}$ margin of error and sufficiently capturing the reported temperature increases.

Three-time metrics were recorded: point cross time, the duration for the heat pack to fully traverse P3; sense time, the delay between crossing P3 and the onset of the temperature spike; and total cross time, the time taken to traverse the entire 70 cm path.

To minimise thermal interference from handling, the heat pack was moved using a thin hook attached to a loop on its tag, ensuring all operator contact remained outside the camera's field of view. Trials were performed at six discrete total cross times between 10 seconds and approximately 0.35 seconds.

2.3 Lateral Motion Analysis Method

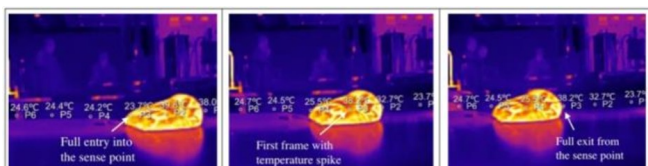


Figure 1 – Diagram of showing how the lateral motion recordings were analysed to gain meaningful data.

The analysis of the lateral motion videos aimed to quantify and explicate the camera's response delay in detecting temperature changes under motion. The individual frames of each of the relevant recordings were extracted and indexed numerically (e.g. Frame_0001 has frame number 1). For each run at each speed, three particular frame numbers were of interest (Figure 1):

- Frame_{entry}, the first frame where the sense point was fully positioned over the object
- Frame_{spike}, the first frame displaying a temperature spike at the sense point
- Frame_{exit}, the first frame when the object had fully passed the sense point

The camera had a reported frame rate of 25Hz. Two key time-based metrics, the sense time and the point cross time, could therefore be calculated as:

$$\text{Sense Time} = \frac{1}{25} \times (\text{Frame}_{\text{spike}} - \text{Frame}_{\text{entry}}) \text{ Point}$$

$$t \text{ Point Time} = \frac{1}{25} \times (\text{Frame}_{\text{exit}} - \text{Frame}_{\text{entry}})$$

These values describe the time between the object passing through the sense point and the thermal sensor registering

temperature spike, and the duration the object remained over the sense point.

3. Results and Discussion

3.1 Forward Motion

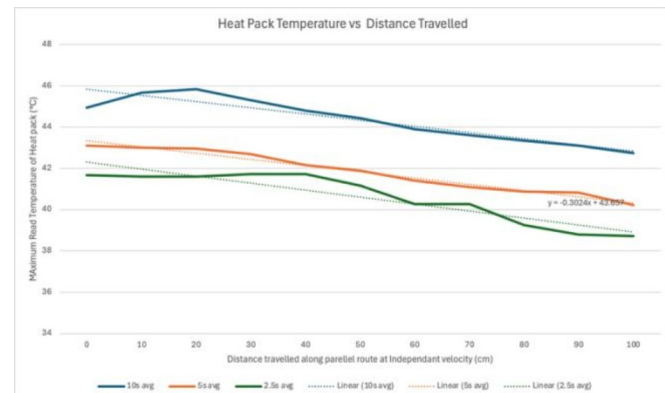


Figure 2 – Graph of the distance travelled by the heat signature against the maximum recorded temperature.

Note that data was collected sequentially, beginning with the 10 second intervals and without replacing the heat pack from any of the nine runs (three repeats of three intervals). As both the 0cm and 100cm points were taken with the pack at a standstill (velocity of 0), the disparity between temperature values is associated with the pack gradually losing energy to its surroundings between runs rather than the velocity during the pack's movement affecting the accuracy of the reading. For each time interval, the heat pack at the end of the 100cm interval read approximately 2.5 degrees cooler than it did at the beginning. The equation for this trend is shown by the equation in Figure 2, this equation was modelled upon the 5s interval runs as it fitted the linear trend the most tightly. Given that the camera was situated a further 23cm away from the zero-centimetre point of the interval, theoretically a room temperature reading of 20°C would be achieved at a certain distance:

$$Y = -0.3024x + 43.657$$

$$X = \frac{20 - 43.657}{-0.3024}$$

$$= 78.23 + 2.3$$

$$= 805.308 \text{ cm}$$

Excel treats x as the number of points taken, which in this case were every decimetre, such that the 23cm extra is an additional 2.3 dm. Extrapolating this trend back to the camera suggests that the temperature of the heat pack for while the five second interval data was collected would've been:

$$Y = -0.3024(-2.3) + 43.657$$

$$Y = 44.35252$$

The existence of this trend suggests that there is a specific distance at which the camera operates most effectively. Having an object of controlled temperature would have been useful for identifying the distance at which the camera operated most accurately. A physical thermometer would not work as effectively because there would be no way to easily to identify the warmest sections of the pack's surface as the camera does.

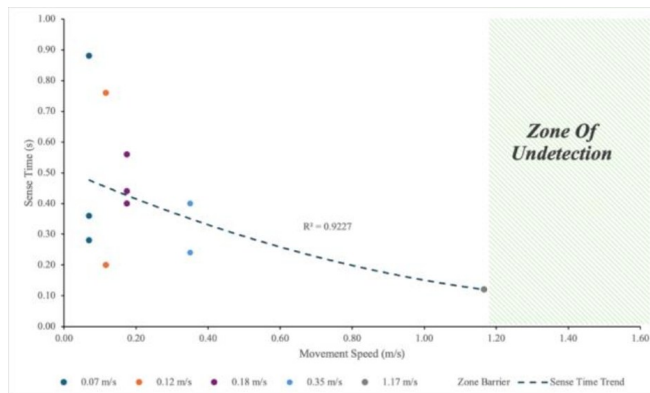


Figure 3 – Graph of movement velocity against sense time.

3.2 Lateral Motion

Figure 3 shows that for lateral object movement speed less than 1.17m/s, the camera sensed a temperature change more quickly as the object's velocity increased. Beyond this speed, the sense point did not record a temperature spike at all, indicating a complete failure of detection. This zone, defined as the zone of 'undetection', constitutes the speed above which our heated object went undetected by our sense point.

This relationship of faster speeds resulting in lower detection times is unexpected. Theoretically, as the slower moving object remains within each pixel's field of view for a longer duration, it was expected for the camera to accumulate more thermal signal to record a stronger and more stable temperature reading. In contrast, a fast-moving object may not give the sensor enough time to detect and respond if only present for 1-2 frames. Hence the most logical explanation for this unexpected relationship is that when the heated object moved quickly across the camera's field of view, it may have caused an abrupt spike in infrared radiation which was more noticeable to the camera than lower speed runs as the ratio of signal to background noise was increased.

The median sense time for all successful detections was 0.37s. Significant variability however was seen across runs, particularly at lower speeds. Standard deviation in sense time was highest for the two slowest speeds (0.07m/s and 0.12m/s) at 0.326 and 0.323, respectively, with corresponding relative standard deviations (RSDs) of 64% and 84%. Faster successfully detected runs exhibited less variability, with runs at speeds 0.18m/s and 0.35m/s reporting RSDs of 18% and

27%. This shows that slower movement speed not only resulted in higher sense time but also greater absolute and relative sense time variation. This variation can be attributed to fluctuations in object emissivity, ambient thermal noise, and possible inconsistencies in object trajectory relative to the sensors focal point during the experiment.

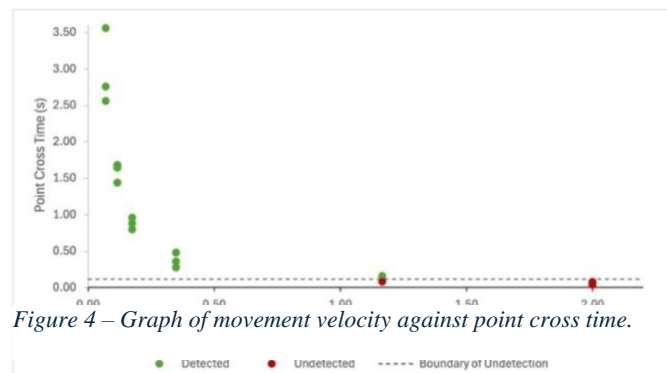


Figure 4 – Graph of movement velocity against point cross time.

The boundary of 'undetection', as seen in Figure 4, represents the boundary point cross time at which no object crossing in lesser time was detected by our camera. The minimum time the camera took to sense a temperature spike was 0.12 seconds (3 frames after object crossed the sense point). This is the point at which our previously consistent trend of greater motion speed corresponding to lower sense times abruptly fails, and no temperature spike at all is recorded.

The presence of this boundary suggests that a heated object can pass through the camera's frame without setting off a temperature spike at high enough speeds. Consequently, systems that rely on detecting a temperature spike to set off a trigger, may fail to register a fast-moving heated object, despite its presence in the frame. Our data suggested that any object crossing the sense point in less than 0.12 seconds (3 frames) avoided causing a temperature spike in the sense point and therefore avoided detection. This may be due to the inability for the IR radiation emitted by the object to accumulate significantly within the sensor's thermal detection threshold within its brief exposure period.

These findings are highly pertinent for industrial applications. A camera set to detect a heated object (intruder, wild animal etc) may fail if the heated object is not detected by the camera's sense point and thus doesn't set off a trigger.

Table 1 – Speed required for different sized objects to avoid detection at a distance of 1.1 meters and detection boundary of 0.12 seconds.

Object (Length)	Speed Required to Avoid Detection (m/s)	Speed Required to Avoid Detection (km/h)
Heat Bag (0.2m)	1.8	6.6
Human (0.4m)	3.6	13
Large Dog (0.7m)	6.4	23
Car (4.9m)	45	160

Table 1 displays the speed required of various everyday heated objects to avoid detection by our thermal camera at a distance of 1.1 metres. This highlights an important overlooked limitation of detection that must be considered in industrial application

3.3 Combined Interpretation and Implications

Both the forward and lateral motion experiments demonstrated the importance of motion speed and direction in influencing infrared camera thermal detection. The experiment was limited in that there was little empirical analysis into the interaction of these two effects.

In the lateral experiment, the threshold speed for undetection was found to be 1.17m/s at a fixed camera distance of 1.1m. Beyond this speed, no temperature spike was observed. However, it is likely that this boundary is not only affected by object size, but also the object's distance from the camera. However, it is likely that this boundary is not only affected by object size, but also the object's distance from the camera.

Firstly, a distant object occupies fewer pixels in the camera's field of view. Consequently, at the same physical speed, a distant object traverses each pixel faster, thus reducing its likelihood of detection. This means more distant objects may avoid detection even at lower speeds than those observed at 1.1m. In effect, the objects in Table 1, positioned greater than 1.1m away from the camera, would be capable of avoiding detection at even lower speeds.

Secondly, as illustrated in the forward motion experiment, thermal signatures at a distance becomes increasingly diffuse relative to the background. It was calculated that our heat pack would fail to register a distinct signature at a distance of 805.308cm. This limiting distance, calculated above for our heat pack, is relative to the size of the 2D projection of the object in question. At this limiting distance an object would go undetected regardless of lateral motion.

Together, these findings suggest that for a given object size and temperature there exists a two-dimensional detection

boundary, defined by both distance and speed. If an object stays below this boundary, in either dimension, it can avoid detection. This offers a valuable framework for describing thermal camera limitations in surveillance applications and beyond.

4. Conclusion

The research undertaken provides insight into the effectiveness of IR cameras detecting objects in motion, especially in a security and surveillance context. Through tests simulating forward motion, it was found that the IR camera was effective in tracking the location and measuring the temperature of the heat signature in motion. However, it was discovered that the recorded temperature experienced a gradual, but significant decrease as the distance between the IR camera and heat signature increased. On average, a 2.5 °C decrease in temperature was recorded 1m further away from the camera. The tests simulating lateral motion measured the sensing time of temperature spikes due to the heat signature and found in all cases that a temperature difference was detected, it took a minimum of 3 frames (i.e. 0.12s) for a change to be recorded. This test also concluded that, contrary to the hypothesis, a faster moving heat signature resulted in a smaller temperature spike sensing time by the IR camera. Most notably, the lateral test confirmed the existence of a critical speed beyond which the IR camera could no longer detect the heat signature. This threshold was determined to be greater than 1.17m/s. As a result, IR cameras were found to be a generally effective security tool but have notable limitations in detecting dynamic heat signatures. To improve the reliability of such systems, optimal camera positioning should be considered, as the closer a heat signature is, the greater the temperature spike recorded by the camera will be. Also, avoiding lateral movement of heat signatures relative to the sensor increases the likelihood of detecting fast-moving objects. This limitation can also be addressed by deploying additional cameras focused on the same area. Finally, while this study measured the effectiveness of InfiRay cameras, other thermal camera brands on the market such as Hikmicro and FLIR, may perform better with dynamic heat signatures or possess greater framerates. A future comparison of different cameras in security settings would prove a worthwhile study.

References

Bhusal, S. (n.d.). Object Detection and Tracking in Wide Area Surveillance Using Thermal Imagery. <https://doi.org/10.34917/8220085>

Biosystems heat and mass transfer—ScienceDirect. (n.d.). ScienceDirect. Retrieved May 25, 2025, from <https://www.sciencedirect.com/science/article/abs/pii/B97801203779000030>

Cansiz, A. (2018). 4.14 Electromechanical energy conversion. In I. Dincer (Ed.), *Comprehensive Energy Systems* (pp. 598–635). Elsevier. <https://doi.org/10.1016/B978-0-12-809597-3.00425-9>

Conduction heat transfer—An overview | ScienceDirect Topics. (n.d.). ScienceDirect. Retrieved May 23, 2025, from <https://www.sciencedirect.com/topics/engineering/conduction-heat-transfer>

Davis, J. W., & Sharma, V. (2004). Robust detection of people in thermal imagery. *Proceedings of the 17th International Conference on Pattern Recognition*.

Gade, R., & Moeslund, T. B. (2014). Thermal cameras and applications: A survey. *Machine Vision and Applications*, 25(1), 245–262. <https://doi.org/10.1007/s00138-013-0570-5>

Havens, K. J., & Sharp, E. J. (2016). Chapter 8—Imager selection. In K. J. Havens & E. J. Sharp (Eds.), *Thermal Imaging Techniques to Survey and Monitor Animals in the Wild* (pp. 121–141). Academic Press. <https://doi.org/10.1016/B978-0-12-803384-5.00008-7>

Heat transfer. (n.d.). NASA Glenn Research Center. Retrieved May 24, 2025, from <https://www.grc.nasa.gov/www/k-12/airplane/heat.html>

Ibrahim, S. (2016). A comprehensive review on intelligent surveillance systems. *Engineering Science and Technology, an International Journal*, 19(1), 22–31. <https://doi.org/10.1016/j.estch.2016.05.004>

Infrared radiation—An overview | ScienceDirect Topics. (n.d.). ScienceDirect. Retrieved May 24–25, 2025, from <https://www.sciencedirect.com/topics/physics-and-astronomy/infrared-radiation>

Krišto, M. (2016). Review of methods for the surveillance and access control using the thermal imaging system. *Review of Innovation and Competitiveness: A Journal of Economic and Social Research*, 2(4), 71–91. <https://doi.org/10.32728/ric.2016.24/5>

Leykin, A., & Hammoud, R. (2006, June). Robust multi-pedestrian tracking in thermal-visible surveillance videos. In *2006 IEEE Computer Society Conference on Computer Vision and Pattern Recognition (CVPR) – Workshops* (p. 136).

Mamat, H. (2019). Nanofluids: Thermal conductivity and applications. In *Reference Module in Materials Science and Materials Engineering*. Elsevier. <https://doi.org/10.1016/B978-0-12-803581-8.11569-3>

Thermal cameras and applications: A survey | Machine Vision and Applications. (n.d.). SpringerLink. Retrieved May 25, 2025, from <https://link.springer.com/article/10.1007/s00138-013-0570-5>

Thermal sensors—Department of Informatics. (n.d.). University of Oslo. Retrieved May 25, 2025, from <https://www.mn.uio.no/ifi/english/research/projects/mecs/sensing/thermal-sensors>

Vollmer, M. (2021). Infrared thermal imaging. In K. Ikeuchi (Ed.), *Computer Vision: A Reference Guide* (pp. 666–670). Springer International Publishing. https://doi.org/10.1007/978-3-030-63416-2_844

Zhao, J., & Cheung, S. C. S. (2009). Human segmentation by fusing visible-light and thermal imagery. *IEEE 12th International Conference on Computer Vision Workshops*.

Zin, T. T., Takahashi, H., & Hama, H. (2007). Robust person detection using far infrared camera for image fusion. *Second International Conference on Innovative Computing, Information and Control*.